Verification of Signal Matching Analysis of Pile Driving Using a Finite Difference Based Continuum Numerical Method

Shahram Feizee Masouleh[1], **Kazem Fakharian**[1,*]

Received 2 September 2007; accepted 9 June 2008

Abstract *: A finite-difference based continuum numerical model is developed for the pile-soil dynamic response during pile driving. The model is capable of simulating the wave propagation analysis along the pile shaft and through the soil media. The pile-soil media, loading and boundary conditions are such that axisymmetric assumption seems to be an optimized choice to substantially reduce the analysis time and effort. The hydrostatic effect of water is also considered on the effective stresses throughout the soil media and at the pile-soil interface. The developed model is used for signal matching analysis of a well-documented driven pile. The results showed very good agreement with field measurements. It is found that the effect of radiation damping significantly changes the pile-soil stiffness due to the hammer blow. The pile tip response shows substantial increase in soil stiffness below and around the pile tip due to driving efforts.*

Keywords*: pile driving analysis, stress wave propagation, continuum numerical model, finite difference method, signal matching analysis, viscous damping, radiation damping.*

1. Introduction

Determination of axial bearing capacity of piles is still an issue in geotechnical engineering practice. Randolph [1] states that "Despite the fact that pile design approaches have advanced enormously within the past few decades, but yet, the most fundamental aspect of pile design, that of estimating the axial bearing capacity, relies heavily on empirical correlations". Different classes of methods have been used by engineers that may be summarized in four groups [2]: (1) static analysis methods, (2) direct application of *in-situ* test methods (such as SPT, CPT…), (3) static load tests, and (4) dynamic (test/analysis) methods.

The main objective of dynamic methods has been to establish a relationship between the blow counts and the axial capacity of the pile. The dynamic methods include application of dynamic formulas, one-dimensional wave equation analysis in piles (WEAP) based on Smith model [3], pile dynamic test (PDA), and signal matching analysis (such as CAPWAP). Signal matching analysis is recognized to be the most reliable dynamic method in practice. The conventional method, however, uses mass-spring-dashpot system [4, 5] to model the surrounding soil and the soil media below the tip (Fig. 1), therefore, imposes some limitations. Pile is a continuum body having infinite number of degrees of freedom surrounded by a continuum media that is soil. In the mass-spring system, the boundary conditions are different than the real system, causing deviations in the system response. Also the effect of soil inertia (also called "radiation damping" or "geometrical damping") can not be easily considered.

Some attempts were made to improve the Smith model such as that proposed by Randolph and co-workers [6,7]. Viscous damping and radiation (inertial) damping were distinguished in the recent models, as opposed to Smith model in which only one damping parameter is introduced in the model. The interface of soil-pile model is modeled by plastic slider and viscous dashpot and the surrounding soil is modeled by elastic spring in parallel with the inertial dashpot, as shown in Fig. 2. Therefore, the dynamic response of the pile-soil interface can be calculated from Eq. 1:

$$\tau = G\left(\frac{w}{d} + \frac{v}{v_s}\right) \le \tau_{lim} \qquad (1)$$

in which G is the soil shear modulus, d is pile diameter ,v_s is the shear wave velocity in soil, and w and v are respectively, displacement and velocity of soil next to the pile-soil interface.

* *Corresponding author. Fax: +98 21 22 27 2000*
Email address: kfakhari@aut.ac.ir (K. Fakharian)
[1] *Department of Civil and Environmental Engineering, Amirkabir University of Technology, Tehran 15875, Iran*

The interface is modeled using a limiting shaft resistance that is a function of relative velocity between pile and soil (Δv) as follows:

$$\tau_{lim} = \tau_s \left[1 + m \left(\frac{\Delta v}{v_0} \right)^n \right] \quad (2)$$

The τ_s is the limit static resistance of the pile shaft, m and n are viscous parameters, and v_0 is usually assumed to be 1 m/s for simplicity. Similar equations for τ_{lim} are proposed by other researchers [8, 9, 10], in which they have specified n equivalent to 0.2 and m is proposed between 0.1 for sand up to 1 for clay.

Some other studies have used so-called continuum numerical methods, mostly finite element method, so that the soil media around the pile shaft and below the pile tip are directly considered in the model [11, 12, 13 and 14]. No comparisons have been, however, made between their predictions and a real-life pile driving data and in their conclusions, it was suggested to verify the predictions of the FEM model against actual pile driving data.

This paper presents a so-called continuum numerical model to improve the limitations of the mass-spring-dashpot system. A finite difference model is used here with axisymmetric assumption for the analysis of pile driving. A signal matching procedure (similar to CAPWAP) was followed by changing the strength and deformation parameters of soil and interface between pile-soil. The fine-tuned parameters were then used to simulate the static axial load-displacement response to be compared with the real test results. In order to overcome the shortcomings of the numerical model to simulate the viscous damping at the soil-pile interface, Eq. 2 is somehow implemented in the numerical model.

2. Case study pile

The case pile is selected from an elaborate pile testing research project along with the "4th International Conference on the Application of Stress-wave Theory to Piles" held in Netherlands, 1992 [15, 16]. Several precast concrete piles were

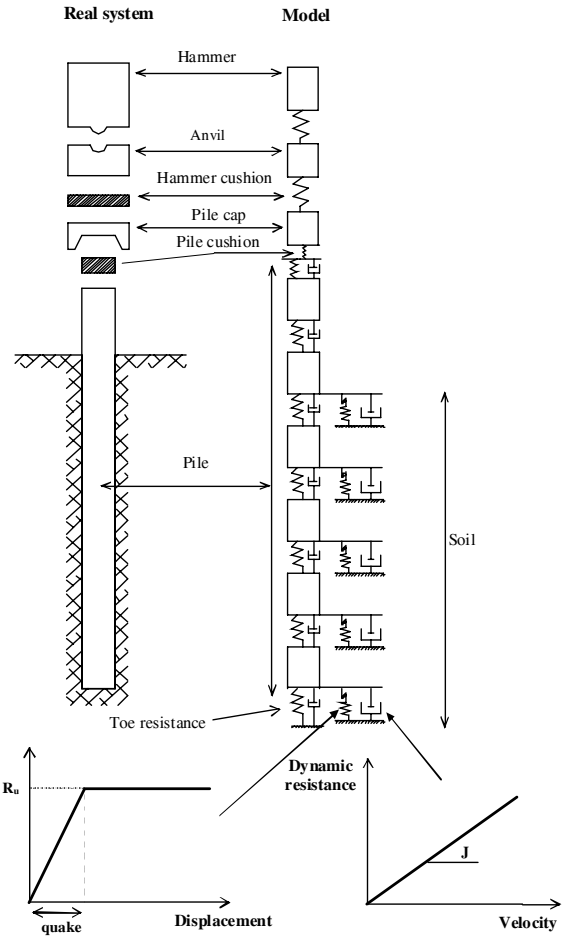

Fig. 1 Pile-soil-hammer system based on Smith model [3].

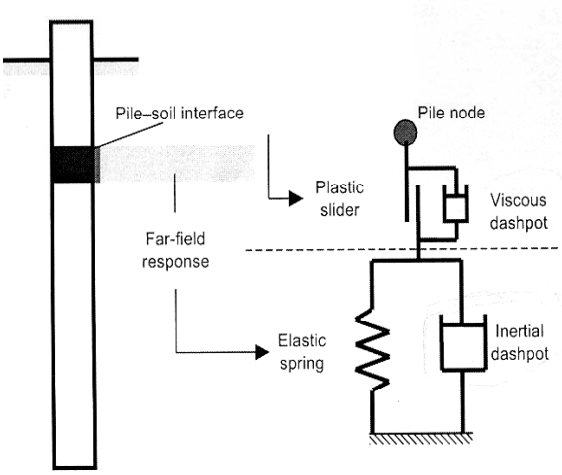

Fig. 2 Dynamic soil-pile shaft model to account for inertial damping [1].

driven at the test site behind the auditorium of Delft Technological University. Static and dynamic test results are available for the selected test pile used in this study.

The soil profile of the site together with CPT results are shown in Fig. 3. The GWT is 1 m below the ground surface. The pile is precast square concrete with 0.25 m dimension and elastic modulus of 36,000 MPa. The 19 m long pile was driven by a hydraulic hammer ICE SC-40, to an embedment depth of 18 m. The blow counts for the last 1 m of driving for 25 cm penetrations are 37, 29, 32 and 41, respectively. The force (F) and velocity (Zv) signals recorded by installing strain gages and accelerometers at 1 m below the pile head and related to the last blow at the end of pile driving are available. The results of a static load test performed after 3 weeks of the initial driving is also available.

2.1. The numerical model

A finite difference scheme is adopted to simulate an axisymmetric model for pile driving analysis, using FLAC-2D version 4. This software is developed on the basis of Lagrangian calculation which is adequate for large deformation modeling. One of its advantages is possibility of modeling large systems with a limited memory, as no stiffness matrix is required (as opposed to FEM, for example). In addition, large deformations do not significantly increase the run-time as no stiffness matrix updates are required after each load or time increment.

In order to benefit from the axisymmetric feature of the 2D numerical model, a 0.3 m diameter pile is assumed having an average correlation with both the cross section area and the circumferential area of the main pile, as shown in Fig. 4. The pile tip has penetrated about 3 m into a medium dense to dense sand (so called Pleistocene sand). Except a 4 m thick clay and peat layer (#2) along the shaft, rest of the layers are mostly sand, but with relatively low q_c values from CPT test (q_c < 12MPa). The boundary distances in horizontal and vertical directions, from shaft and pile tip, respectively,

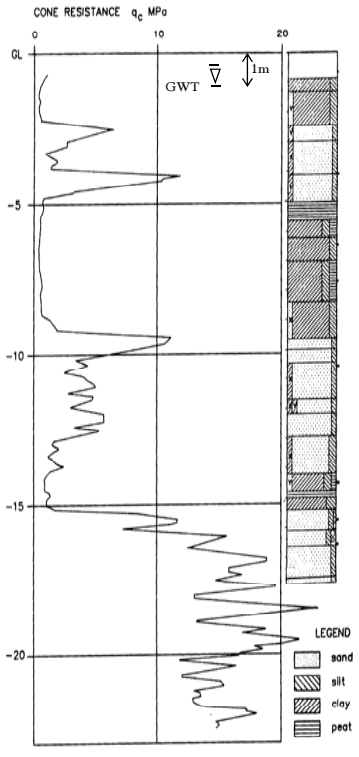

Fig. 3 Soil profile and CPT results [16].

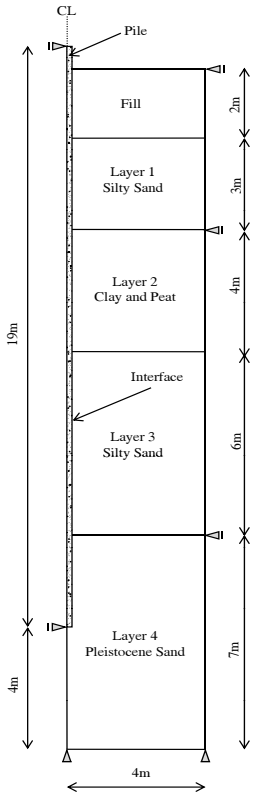

Fig. 4 Axisymmetric pile-soil model for pile driving simulation.

are 4 m in the axisymmetric mesh. The selected distances are far enough to minimize the stresses resulted and propagated from pile driving [17]. In accordance with the highest stress gradients near pile shaft and the soil around the pile tip, the mesh sizes are specified 5 × 5 cm within 2 m distance from shaft and tip, and 10 × 10 cm outside this zone to the vertical and horizontal boundaries (Fig. 5). Interface elements between pile shaft and soil are inserted to facilitate the pile-soil slip during driving. The Mohr-Coulomb failure criterion is used for the interface, on the basis of which slip between soil and pile occurs, if the generated shear stress during driving exceeds the shear strength.

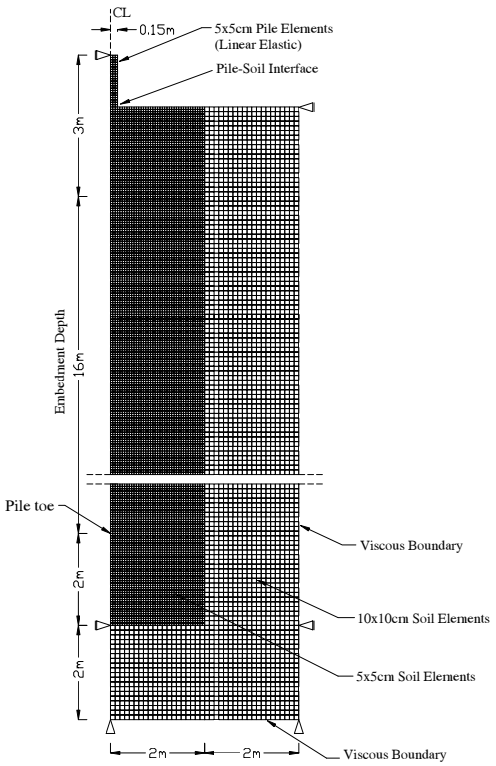

Fig. 5 Finite difference mesh for the axisymmetric pile-soil model.

As a result of hammer blow on the pile head, part of the stress wave enters and propagates within the surrounding soil. The degree and magnitude of the penetrated energy depends on the interface and the pile-soil mechanical parameters [18]. In real pile driving, the penetrated stress waves propagate away from the pile and dissipate gradually, which is referred to as "radiation damping". As the model boundaries have limited distance from the pile, viscous boundaries are assumed at the vertical and bottom horizontal boundaries to absorb such waves and prevent their reflection. Dampers in two perpendicular directions are implemented at each boundary node as proposed by Lysmer [19].

An elasto-perfectly plastic model with Mohr-Coulomb failure criterion is used for the soil material. The required mechanical parameters for each soil layer are estimated on the basis of CPT results with common correlations available in literature [20]. The estimated parameters are presented in Table 1. The cohesion and Poisson's ratio are assumed 10 kPa and 0.4, respectively, for all the four layers. The low value of cohesion assumed for all layers is to account for a limited amount of cementation in the soil layers.

A two-phase media is considered for soil to include the hydrostatic effect of water. Therefore, the effective stresses are involved in the soil as well as the soil-pile interface during the analysis. As most of the layers (except the 4-m layer 2) along the pile shaft are sand with high permeability, drained analysis is adopted

Table 1 Soil parameters for different layers from CPT correlations

Soil layer	Friction angle	Cohesion (kPa)	Elastic modulus (MPa)	Poisson's ratio	Density (kN/m^3)
1	36	10	20	0.4	**19**
2	20	10	20	0.4	**19**
3	30	10	20	0.4	**19**
4	36	10	40	0.4	**19**

throughout the pile-soil response. Therefore, the pore-pressure built-ups in the numerical model is not activated. This is in fact not the main concern in this research, as only one hammer blow is simulated during which the pore pressure variations may not be significant.

One of the shortcomings of most of the numerical models is their incapability in considering the effects of viscous damping at the soil-structure interface. This rate-dependent property causes increase in shear strength at the pile-soil interface due to the high relative velocity, in excess to that of the static shear resistance. It has been attempted to implement Eq. 2 in the numerical model to include the effects of viscous damping.

As explained before, interface elements are used at the soil-pile contact surface to facilitate the slip of pile with respect to the soil. The important parameters in static analysis for interface are shear stiffness, normal stiffness, and soil shear strength parameters. If the shear stress at the interface exceeds the Mohr-Coulomb static shear strength, then slip occurs at the pile-soil contact surface. The FLAC cannot, however, account for the rate dependent viscous effects at the interface. To facilitate this effect, the ultimate (or limit) shear strength is defined as the rate-dependent τ_{lim} of Eq. 2. This was added to the numerical model through its FISH programming option. The m and n were assigned a value of 0.2 [1, 7] and the pile was subjected to the input hammer impact force for the dynamic analysis.

2.2. Signal matching analysis

Stage construction option has been used to consider the effect of gravitational stresses during the analysis. In the first step, the soil layers are allowed to reach equilibrium under self-weight stresses, and then the resulted deformations are set to zero. In the second step, the interface elements with zero shear strength are considered between pile-soil to allow the pile to displace freely under self-weight. For performing the pile driving dynamic analysis, the recorded force-time at strain gage location on the pile (resulted from pile driving) is input on the pile, and then the velocity signal is calculated from the analysis. The calculated Zv at the gage location is compared with the measured Zv, and if not matched, efforts are made in subsequent analyses by trial and error, similar to the CAPWAP type analyses, to match the signals.

The measured force, measured Zv, and the fine-tuned computed Zv are shown in Fig. 6. The most important influencing time domain for the shaft resistance adjustments is between peak force (or velocity) to 2L/C (about 9.5 ms in the study case). Therefore, trial and error were made to match the computed and measured velocity signals, by adjusting the interface strength (angle of friction and cohesion) and deformation parameters (normal and shear stiffness) for different layers. The final parameters are presented in Table 2.

In order to adjust the pile tip effects in the signal matching process, the soil strength (angle of friction and cohesion) and deformation (elastic modulus and dilation angle) parameters were adjusted in a limited zone around the pile tip. Local damping parameters considered for the pile and soil are 3% and 5%, respectively. The final parameters adjusted for soil surrounding the pile tip are presented in Table 3.

3. Results

Tables 2 and 3 present the final interface and soil parameters, to achieve a reasonable match between the measured and computed Zv signals shown in Fig. 6. The parameters obtained for around and below the pile tip from signal

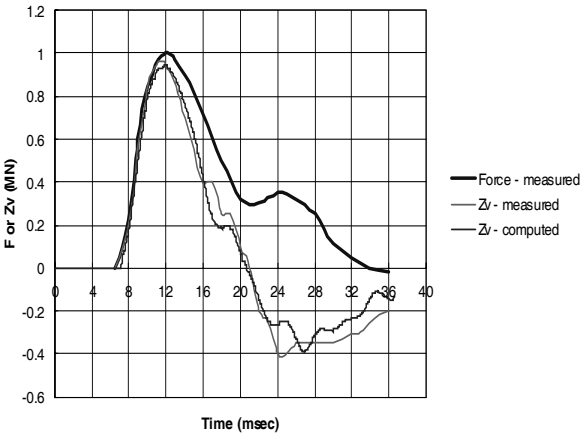

Fig. 6 Measured force, and measured and computed Zv wave traces.

Table 2 Interface strength and deformation parameters from signal matching analysis

Soil layer	Interface strength parameters		Interface deformation parameters	
	Friction angle	Cohesion (kPa)	Shear stiffness, k_s (kN/m^3)	Normal stiffness, k_n (kN/m^3)
1	5	0	50,000	5,000,000
2	5	0	50,000	5,000,000
3	26	10	50,000	5,000,000
4	32	10	50,000	5,000,000

Table 3 Strength and deformation parameters of soil around pile tip from signal matching analysis

Soil block dimensions below pile tip	Strength parameters		Deformation parameters	
	Friction angle	Cohesion (kPa)	Dilation angle	Elastic modulus (MPa)
105 × 105 cm	45	50	5	500

matching analysis (Table 3), indicate high magnitudes for strength parameters (E of 500 MPa). This is attributed to the fact that the pile tip is embedded in a sandy deposit having a high densification potential during the driving efforts. On the basis of an analytical study by Yang [21], the influence zone limit of an axially loaded pile in clean sand and compactable silty sand are 3.5D-5.5D and 1.5D-3D, respectively. The signal matching trial and error efforts indicated that a cube with depth 3.5D (105 cm) below the pile tip elevation is providing a good match. The cube depth is in accordance with the influence zone ranges proposed by Yang [21] for the silty sand.

In order to investigate the other aspects of the system response, further results are presented and discussed below.

The applied energy to the pile head due to hammer impact is computed versus time and compared with the measured energy (Enthru) from dynamic testing as shown in Fig. 7. The Enthru was computed using Eq. 3 which is in fact the accumulation of force multiplied by displacement at the elevation of attached gages. The displacement is in fact calculated from v.dt.

$$W = \int_0^t F.v.dt \tag{3}$$

The peak energy is attained at time 2L/C after

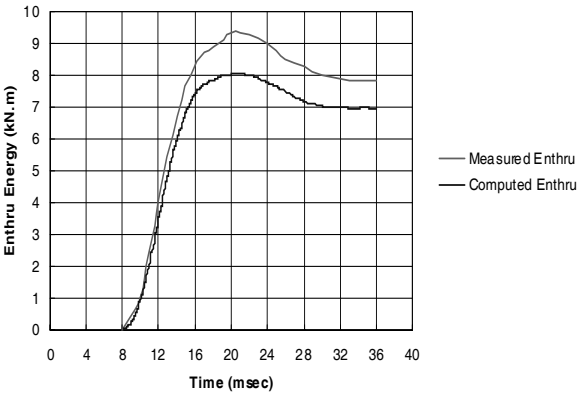

Fig. 7 Measured and computed applied energy (Enthru) versus time.

which the energy is decreasing and eventually approaching a residual value at about 36 ms. Thereafter, the energy is constant as the force and velocity are almost zero. The reduction of energy between peak to residual is attributed to elastic rebound of the pile tip and shaft, known in practice as soil quake. A good correlation is observed between the two measured and computed curves, indicating a good signal matching effort.

The pile head and tip displacements with time for the impact blow resulted from signal matching analyses are shown in Fig. 8. The difference between the two curves at peak (about

3.5 mm) is equivalent to the pile elastic compression, which is eliminated when the permanent displacement after 36 ms has reached. The figure also shows that the permanent displacements at both tip and head are 4.6 mm. The reported average penetration per blow during driving in the last 25 cm is 6 mm (41blows/25cm) that shows a relatively good correlation with the computed 4.6 mm permanent penetration. The other important observation in Fig. 8 is the elastic pile tip displacement of 2.5 mm (difference between pile tip peak displacement and the permanent displacement). This 2.5 mm displacement is in fact the same as, so-called, toe (tip) quake that has been suggested by Goble et al. [22] to be considered as D/120 that compares very well with the calculated value in which D is the pile diameter.

It would be also important to investigate the effect of radiation (or inertial) damping on the pile response to the hammer impact. A sample result is presented in Fig. 9 indicating the mobilized shear stress at pile-soil interface 6 m above the pile tip (mid layer 3) with respect to the pile vertical displacement at that elevation. The result of the static response (discussed in subsequent parts of this section) is presented together with dynamic response. Comparison between static and dynamic responses clearly shows the effect of radiation (or inertial) damping. It is observed that the radiation damping causes substantial increase in the system response (around 4 times) and hence considerable decrease in shaft quake (displacement at which soil reaches the limit stress).

The effect of the radiation damping on the pile tip response is presented in Fig. 10. It is observed that the radiation (or inertial) damping has caused increase in both stiffness (around 1.7 times) and the force at the pile tip.

The last part of the presented results includes comparison between static load test results and static response predictions. Figure 11 shows the static axial load versus pile head displacement both from the static load test in the field and the simulated results by the numerical model. The analysis was performed using the same strength and deformation parameters obtained for soil and interface, from signal-matching analyses described in the former subsections. It is observed in Fig. 11 that up to a pile head displacement of 30 mm, a reasonably good correlation exists between prediction and static load test. Assuming a failure criterion for the pile at a displacement equivalent to 10% of the pile tip diameter, or in fact 30 mm, the ultimate pile capacity is scaled off as 1200 kN. This is indicating the reasonable accuracy of the numerical model in the static capacity prediction. The distribution of the shear stress on the pile shaft on the basis of the static load test simulation is shown in Fig. 12. The tip and shaft resistances are thus obtained as 700 kN and 500 kN, respectively. The trend of shear stress variations on the pile shaft compares reasonably well with the q_c variations of the CPT profile of Fig. 3.

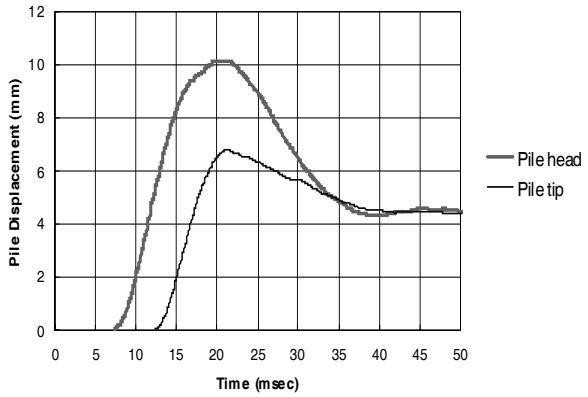

Fig. 8 Pile head and tip displacements versus time.

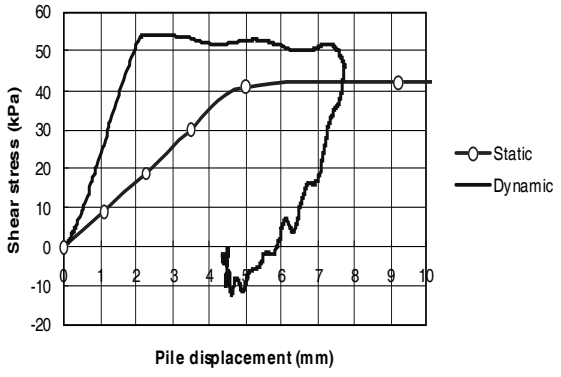

Fig. 9 Static and dynamic shaft response at 6m above tip.

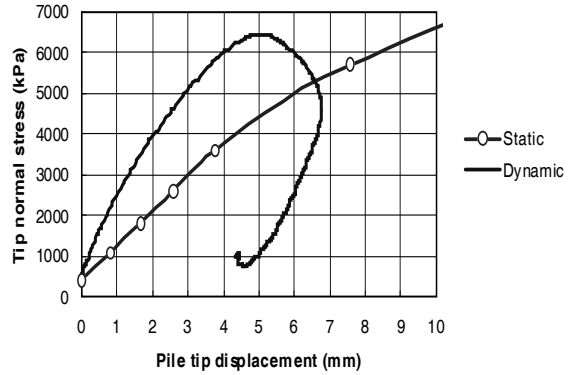

Fig. 10 Static and dynamic toe response.

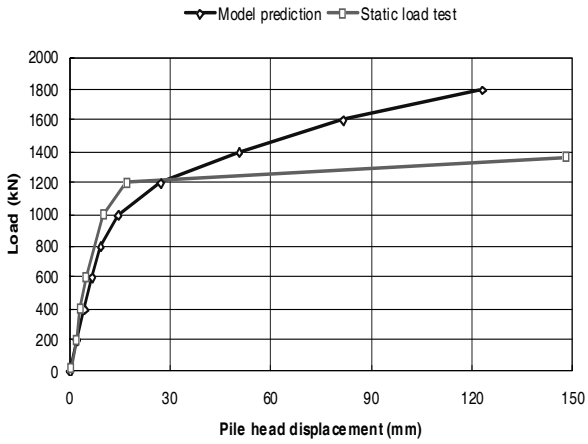

Fig. 11 Static load test simulation result compared with the real test result.

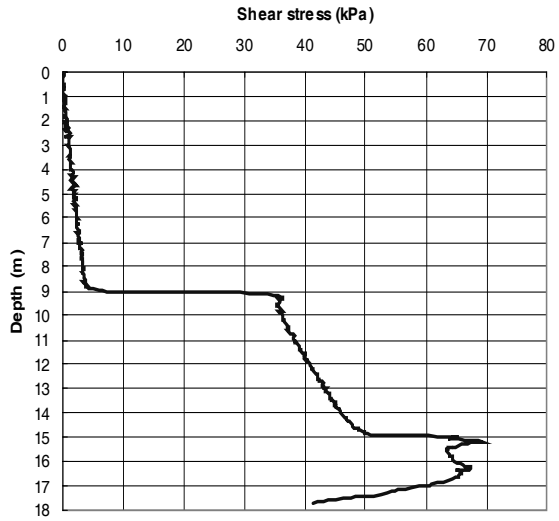

Fig. 12 Calculated distribution of shear stress on the pile shaft; compares reasonably good with the CPT profile.

4. Conclusions

A finite difference based continuum numerical model has been developed to simulate the pile driving. Effect of GWT is included in the model to correctly quantify the effective stresses both within the soil media and at the pile-soil interface. Also, the viscous damping effect at the interface is somehow introduced to the numerical model. A signal matching analysis is performed on a well-documented real driven pile and the results are compared with the static load test. The main conclusions of the study are listed below:

- The effect of inertial (or radiation) damping resulted from the surrounding soil is successfully accounted for by the continuum model.

-The results show that the sandy soil below and around the pile tip has substantially densified during driving. Such physical concepts cannot easily be understood in lumped models.

- The signal-matching analysis for a real driven pile was successfully performed in continuum model showing good predictions of Enthru, pile tip quake, static load-displacement response and the load distribution on the pile shaft.

- The viscous damping effects at the pile-soil interface were successfully implemented in the numerical model by varying the shear strength parameters proportional to the velocity variations during pile driving.

- The developed numerical model shows to be a promising tool for more elaborate analyses to further clarify the advantages of a continuum numerical model compared to conventional lumped models.

5. Notations

A: Pile cross section area (m^2)
C: Wave speed in pile (m/s)
D: Pile diameter (m)

E: Elastic modulus (N/m^2)
F: Force (N)
k_n: Interface normal stiffness (N/m^3)
k_s: Interface shear stiffness (N/m^3)
L: Pile length (L)
v: Velocity (m/s)
Z: Impedance (EA/C)
ρ : Mass density (kg/m^3)

6. References

[1] Randolph, M.F. (2003). "Science and Empiricism in Pile Foundation Design." 43rd Rankine Lecture, Geotechnique, 54(1).

[2] Fakharian, K. and Eslami, A. (2006). "Axial Bearing Capacity of Piles." Transportation Research Institute, Ministry of Roads and Transportation, 241 p.

[3] Smith, E.A.L. (1960). "Pile-Driving Analysis by the Wave Equation." Journal of the Soil Mechanics and Foundations Division, 86 (EM 4), 35-61.

[4] Rausche, F. (1970). "Soil Response from Dynamic Analysis and Measurements on Piles." Thesis presented to the Case Western Reserve University, at Cleveland, Ohio, in 1970, in partial fulfillment of the requirements for the degree of Doctor of Philosophy.

[5] Rausche, F., Goble, G.G., and Likins, G. (1985). "Dynamic Determination of Pile Capacity." Journal of Geotechnical Engineering, 111(3), 367-383.

[6] Simons, H. A. & Randolph, M. H. (1985). A new approach to one-dimensional pile driving analysis. Proc. 5th Int. Conf. Numerical Methods in Geomechanics, Nagoya 3, 1457-1464.

[7] Lee, S. L., Chow, Y. K., Karunaratne, G. P. & Wong, K. Y. (1988). Rational wave equation model for pile-driving analysis. J. Geotech. Engng, ASCE 114, No. 3, 306-325.

[8] Litkouhi, S. & Poskitt, T. J. (1980). Damping constant for pile driveability calculations. Geotechnique 30, No. 1, 77-86.

[9] Heerema, E. P. (1981). Dynamic point resistance in sand and in clay, for pile driveability analysis. Ground Engrg., 4(6), 30-46.

[10] Coyle, H. M., and Gibson, G. C. (1970). Empirical damping constants for sands and clays. J. Soil Mech. and Found. Div., ASCE, 96(SM3), 949-965.

[11] Coutinho, A.L.G.A., Costa, A. M., Alves, J.L.D., Landau, L., and Ebecken, N.F.F. (1988). "Pile Driving Simulation and Analysis by the Finite Element Method", Proc. 3rd Int. Conf., Application of Stress-Wave Theory to Piles, May 25-27, 1988, Ottawa, Canada.

[12] Borja, R.I. (1988), "Dynamics of Pile Driving by the Finite Element Method." Computers and Geotechnics, 5(11), 39-49.

[13] Mabsout, M. and Tassoulas, J.L. (1994). "A Finite Element Model for the Simulation of Pile Driving," International Journal for Numerical Methods in Engineering, Vol. 37, pp. 257-278, 1994.

[14] Mabsout, M.E., Reese, L.C., and Tassoulas, J.L. (1995). "Study of Pile Driving by Finite-Element Method." Journal of Geotechnical and Geoenvironmental Engineering, ASCE, 121(7), 535-543.

[15] Geerling, J. and Smits, M. Th. J. H. (1992). "Prediction of load-displacements characteristics of piles from the results of dynamic/kinetic load tests", Proc. 4th Conf. Application of Stress Wave Theory to piles, 12-24 September 1992, Delft University, Netherlands.

[16] Heijnen, W.J. (1992). "General Soil Conditions of the Test Sites", Proc. 4th Conf. Application of Stress Wave Theory to piles, 12-24 September 1992, Delft University, Netherlands.

[17] Feizee S. M. "Evaluation of design parameters of pile using dynamic testing and analyses", Ph.D. thesis, Amirkabir University of Technology, Tehran, Iran.

[18] Nath. B., (1990) "A Continuum Method of Pile Driving Analysis: Comparison with the Wave Equation Method." Computers and Geotechnics 10 (1990) 265-285.

[19] Lysmer, J., and Kuhlemeyer R. L. (1969) "Finite Dynamic Model for Infinite Media." J. Eng. Mech., 95 (EM4), 859-887.

[20] Bowles, J. E., (1996), Single piles: Dynamic analysis, Load tests, Foundation analysis and design, McGraw-Hill.

[21] Yang, J. (2006), "Influence Zone for End Bearing of Piles in Sand." J. Geotech. and Geoenvir. Engrg., Volume 32, Issue 9, pp. 1229-1237.

[22] Goble, G.G., Rausche F., Likins G. and Associates Inc. (1996). "Introduction to GRLWEAP, the 1997-2 GRLWEAPTM PROGRAM", Cleveland, Ohio.